

---

# Extracting Interpretable Logic Rules from Graph Neural Networks

---

**Chuqin Geng**

McGill University  
Mila Quebec AI Institute  
chuqin.geng@mail.mcgill.ca

**Ziyu Zhao**

McGill University  
ziyu.zhao@mail.mcgill.ca

**Zhaoyue Wang**

McGill University  
Mila Quebec AI Institute  
zhaoyue.wang@mail.mcgill.ca

**Haolin Ye**

McGill University  
haolin.ye@mail.mcgill.ca

**Xujie Si**

University of Toronto  
xujie.si@utoronto.ca

## Abstract

Graph neural networks (GNNs) operate over both input feature spaces and combinatorial graph structures, making it challenging to understand the rationale behind their predictions. As GNNs gain widespread popularity and demonstrate success across various domains, such as drug discovery, studying their interpretability has become a critical task. To address this, many explainability methods have been proposed, with recent efforts shifting from instance-specific explanations to global concept-based explainability. However, these approaches face several limitations, such as relying on predefined concepts and explaining only a limited set of patterns. To address this, we propose a novel framework, LOGICXGNN, for extracting interpretable logic rules from GNNs. LOGICXGNN is model-agnostic, efficient, and data-driven, eliminating the need for predefined concepts. More importantly, it can serve as a rule-based classifier and even outperform the original neural models. Its interpretability facilitates knowledge discovery, as demonstrated by its ability to extract detailed and accurate chemistry knowledge that is often overlooked by existing methods. Another key advantage of LOGICXGNN is its ability to generate new graph instances in a controlled and transparent manner, offering significant potential for applications such as drug design. We empirically demonstrate these merits through experiments on real-world datasets such as MUTAG and BBBP.

## 1 Introduction

Graph Neural Networks (GNNs) have emerged as powerful tools for modeling and analyzing graph-structured data, achieving remarkable performance across diverse domains, including drug discovery [12, 21, 28], fraud detection [19], and recommender systems [5]. Despite their success, GNNs share the black-box nature inherent to the neural network family, which poses challenges to their further development in high-reliability applications such as healthcare [1, 4].

To this end, several explainability methods have been developed to uncover the inner decision-making mechanisms of GNNs. However, most of these methods are limited to providing local explanations

tailored to specific input instances or rely on interpretations based on input feature attributions [13, 18, 22, 24, 31]. Another line of research focuses on global explanations that describe the overall behavior of models [2, 3, 30]. These approaches offer more human-readable and precise explanations by leveraging logical formulas and interpretable concepts. However, they have limitations, such as relying on predefined concepts and generating rules that explain only a limited set of patterns within each class without effectively distinguishing between these classes.

To this end, we propose LOGICXGNN, a novel framework that extracts interpretable logic rules to explain the internal reasoning process of GNNs while maintaining classification accuracy comparable to the original model. LOGICXGNN ensures interpretability by grounding the hidden predicates of the rules into the input space using decision trees, which are both computationally efficient and data-driven. To the best of our knowledge, LOGICXGNN is the first *interpretable, rule-based functional equivalent* of GNNs. Additionally, it can function as a *generative model*, with notable potential in fields such as drug design and knowledge discovery. We demonstrate the effectiveness of our approach through extensive experiments on real-world benchmarks, including the IMDB [16], Mutagenicity [6], and BBBP [27] datasets. In summary, we make the following contributions:

- We propose LOGICXGNN, a novel post-hoc framework for extracting interpretable logic rules from GNNs. It models the detailed computational processes in GNNs—such as message passing and pooling—making it model-agnostic, efficient, and fully data-driven.
- Experimental results demonstrate that LOGICXGNN significantly outperforms state-of-the-art global explanation methods in preserving the discriminative power of GNNs, while achieving *10 to 100* times faster overall runtime. As a rule-based classifier, LOGICXGNN can even surpass the original GNNs on well-structured datasets, such as molecular graphs.
- Thanks to its high interpretability and strong alignment with the decision-making processes of GNNs, LOGICXGNN supports effective knowledge discovery—it can extract detailed and accurate knowledge (e.g., chemical) that is often overlooked by existing approaches.
- As LOGICXGNN makes decision-making in GNNs transparent, it can be used as a generative model for creating graph instances, holding significant potential in fields such as drug design.

## 2 Preliminary

### 2.1 Graph Neural Networks

Consider a graph  $G = (V_G, E_G)$ , where  $V_G$  represents the set of nodes and  $E_G$  represents the set of edges. For a collection of graphs  $\mathcal{G}$ , let  $\mathcal{V}$  and  $\mathcal{E}$  denote the sets of vertices and edges across all graphs in  $\mathcal{G}$ , respectively, with  $|\mathcal{V}| = n$ . Each node is associated with a  $d_0$ -dimensional feature vector, and the input features for all nodes are represented by a matrix  $\mathbf{X} \in \mathbb{R}^{n \times d_0}$ . An adjacency matrix  $\mathbf{A} \in \{0, 1\}^{n \times n}$  is defined such that  $\mathbf{A}_{ij} = 1$  if an edge  $(i, j) \in \mathcal{E}$  exists, and  $\mathbf{A}_{ij} = 0$  otherwise. A graph neural network (GNN) model  $\mathcal{M}$  learns to embed each node  $v \in \mathcal{V}$  into a low-dimensional space  $\mathbf{h}_v \in \mathbb{R}^{d_L}$  through an iterative message-passing mechanism over the  $L$  number of layers. At each layer  $l$ , the node embedding is updated as follows:

$$\mathbf{h}_v^{l+1} = \text{UPD}(\mathbf{h}_v^l, \text{AGG}(\{\text{MSG}(\mathbf{h}_v^l, \mathbf{h}_u^l) \mid \mathbf{A}_{uv} = 1\})), \quad (1)$$

where  $\mathbf{h}_v^0 = \mathbf{X}_v$  is the initial feature vector of node  $v$ , and  $\mathbf{h}_v^L$  represents the final node embedding at the final layer  $L$ . The update function UPD, aggregation operation AGG, and message function MSG define the architecture of a GNN. For instance, Graph Convolutional Networks (GCN) [10] use an identity message function, mean aggregation, and a weighted update. In essence, the GNN  $\mathcal{M}$  aggregates information from both the feature space and the topological structure of  $G$  to compute node embeddings, which are then optimized for downstream tasks such as graph classification.

**Graph Classification** Suppose we have a set of graphs  $\mathcal{G}$  and a label function  $f : \mathcal{G} \rightarrow \{1, \dots, C\}$  that assigns one of  $C$  classes to each graph in  $\mathcal{G}$ . To approximate  $f$ , we define a GNN model  $\mathcal{M}$  for graph classification by passing the graph embeddings  $\mathbf{h}_G^L$  to a fully connected layer followed by a softmax function. Here, the graph embeddings are commonly computed by taking the mean of all node embeddings in the graph  $\mathbf{h}_G^L := \text{mean}(\mathbf{h}_v^L \mid v \in V_G)$  through the operation `global_mean_pooling`.

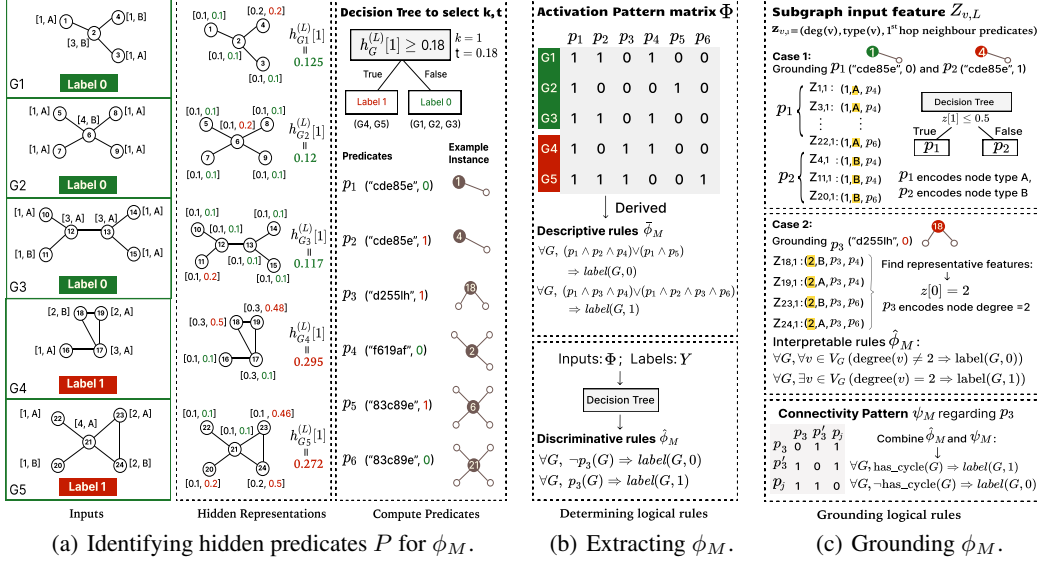


Figure 1: An overview of the LOGICXGNN framework, which involves identifying hidden predicates, extracting rules, and grounding these rules in the input space for interpretability.

## 2.2 First-Order Logic Rules for GNN Interpretability

First-order logic (FOL), also known as predicate logic, is highly interpretable to humans, making it an excellent tool for explaining the behaviour of neural networks [34]. In this paper, our proposed framework, LOGICXGNN, aims to elucidate the inner decision-making process of a GNN  $\mathcal{M}$  using a *Disjunctive Normal Form (DNF)* formula  $\phi_M$ . The formula  $\phi_M$  is a logical expression that can be described as a disjunction of conjunctions (OR of ANDs) over a set of predicates  $P$ , where each  $p_j$  represents a logical condition or property defined on the graph structure  $\mathbf{A}$  and input features  $\mathbf{X}$ . Importantly,  $\phi_M$  incorporates the *universal quantifier* ( $\forall$ ), providing a global explanation that is specific to a class of instances. This makes  $\phi_M$  a rule-based model that is functionally equivalent to  $\mathcal{M}$  - a significant advantage not typically offered by other explanation work. To provide a concrete example of  $\phi_M$ , suppose the model  $M$  is trained to determine whether a molecule  $G$  is soluble. In this case, we may extract the following logical rules  $\phi_M$  from  $M$ :

$$\forall G, (p_1(G) \wedge p_2(G)) \vee (p_3(G) \wedge p_4(G)) \Rightarrow \text{label}(G, s), \quad (2)$$

where  $p_1(G)$  represents "The molecule contains a hydroxyl group (-OH)",  $p_2(G)$  represents "The molecule has a ring structure",  $p_3(G)$  represents "The molecule contains a carbonyl group (C=O)",  $p_4(G)$  represents "The molecule has a high degree of branching", and  $\text{label}(G, s)$  is a predicate indicating that graph  $G$  is assigned the class label  $s$  ("soluble").

While looks promising, extracting such a DNF formula  $\phi_M$  from the original GNN  $\mathcal{M}$  is indeed challenging. More specifically, we need to address the following key questions:

1. How can we identify a set of predicates  $P$  that are both interpretable and critical for classification?
2. How can we determine the logical structure of  $\phi_M$  that not only explains data from a specific class but also effectively rejects data from other classes?
3. Can we design an approach that is both efficient (with minimal computational overhead) and generalizable to different tasks and model architectures?

### 3 The LOGICXGNN Framework

In this section, we show how LOGICXGNN (denoted as  $\phi_M$ ) addresses the aforementioned challenges. For ease of discussion, we divide LOGICXGNN into three critical sub-problems. Figure 1 illustrates an overview of the LOGICXGNN framework.

#### 3.1 Identifying Hidden Predicates $P$ for $\phi_M$

We start by discussing the identification of hidden predicates for graph classification tasks. In fact, since we define hidden predicates at the node level, our framework naturally extends to node classification tasks, as demonstrated in Appendix A.9.

As previously mentioned, the desired predicates  $P$  should capture commonly shared patterns in both graph structures  $\mathbf{A}$  and hidden embeddings  $\mathbf{h}^L$  across a set of instances in the context of GNNs. While graph structure information can be encoded into hidden embeddings, it often becomes indistinguishable due to oversmoothing during the message-passing process [11, 29]. To mitigate this, we explicitly model common patterns in graph structures.

After  $L$  layers of message passing, the receptive field of a node  $v$  corresponds to a subgraph that includes the node itself and its  $1, \dots, L$ -hop neighborhoods. Intuitively, nodes with isomorphic receptive fields tend to exhibit similar properties and may even belong to the same class. Similarly, graph instances sharing multiple isomorphic subgraphs often display related characteristics. To exploit this, we use these subgraphs—nodes’ neighborhoods—to represent structural patterns and use graph hashing to compare and store these patterns efficiently. Formally, the computation of a structural pattern contributed by a certain node  $v$  is given by the following function:

$$\text{Pattern}_{\text{struct}}(v) = \text{Hash}(\text{ReceptiveField}(v, \mathbf{A}, L)). \quad (3)$$

Next, we discuss common patterns in the hidden embeddings. During the training of GNNs for classification tasks, the hidden embeddings are optimized to differentiate between classes. Empirically, we find that a small subset of specific dimensions in the final-layer embeddings  $\mathbf{h}_G^L$  is sufficient to distinguish instances from different classes when using appropriate thresholds, often achieving similar accuracy to the original neural networks. Similar observations have been reported in [7].

In this work, we apply the decision tree algorithm to the collection of final-layer graph embeddings of training data to identify a set of the most informative dimensions  $K$  along with their corresponding thresholds  $T$ . Formally, this is expressed as:

$$\text{DecisionTree}(\{\mathbf{h}_G^L \mid G \in \mathcal{G}\}, \mathbf{Y}) \rightarrow (K, T) \quad (4)$$

where  $\mathbf{Y}$  represents the label vector. We then leverage this information to construct embedding patterns at the node level, aligning with the definition of structural patterns. Recall that  $\mathbf{h}_G^L := \text{mean}(\mathbf{h}_v^L \mid v \in V_G)$ , so we broadcast  $K$  and  $T$  to each node embedding  $\mathbf{h}_v^L$ . For node classification tasks, since  $K$  and  $T$  are already computed at the node level, broadcasting is unnecessary. Then, for an input node  $v$ , its embedding value  $\mathbf{h}_v^L$  at each informative dimension  $k \in K$  is compared against the corresponding threshold  $T_k$ . The result is then abstracted into binary states: 1 (activation) if the condition is met, and 0 (deactivation) otherwise. Formally, we have:

$$\mathcal{I}_k(\mathbf{h}_v^L) = 1 \text{ if } \mathbf{h}_v^L[k] \geq T_k, \text{ else } 0 \quad (5)$$

In summary, for both node and graph tasks, the embedding pattern contributed by a given node  $v$  can be computed using the following function:

$$\text{Pattern}_{\text{emb}}(v) = [\mathcal{I}_1(\mathbf{h}_v^L), \mathcal{I}_2(\mathbf{h}_v^L), \dots, \mathcal{I}_K(\mathbf{h}_v^L)] \quad (6)$$

Putting it together, we define the predicate function as  $f(v) = (\text{Pattern}_{\text{struct}}(v), \text{Pattern}_{\text{emb}}(v))$ . To identify the set of hidden predicates, we iterate over each node  $v \in \mathcal{V}$  in the training set, collect all  $f(v)$ , and transform them into a set  $P$ . In addition, when a node  $v$  is evaluated against a predicate  $p_j$ , the evaluation  $p_j(v)$  is true only if both the structural and embedding patterns from  $f(v)$  match the predicate. To extend the applicability of a predicate to a graph instance  $G$ , we override its definition as follows:

$$p_i(G) = 1 \text{ if } \exists v \in V_G, p_i(v) = 1, \quad p_i(G) = 0 \text{ if } \forall v \in V_G, p_i(v) = 0. \quad (7)$$



To better illustrate the process of identifying hidden predicates, we present a simple example in Figure 1(a). This scenario involves a binary graph classification task, a common setup in GNN applications. In this example, we have five input graphs, with each node characterized by two attributes: degree and type. The types, “A” and “B”, are encoded as 0 and 1, respectively. A GNN with a single message-passing layer is applied, generating a 2-dimensional embedding for each node (i.e.,  $d_L = 2$ ). As only one message-passing layer is used, structural patterns are extracted based on the nodes and their first-order neighbors.

Using decision trees, we identify the most informative dimension  $k = 1$ , and its corresponding threshold  $t = 0.18$  from the graph embeddings. This threshold is then applied to the node embeddings to compute embedding patterns. As a result, six predicates are derived. Notably,  $p_5$  (“83c89e”, 1) and  $p_6$  (“83c89e”, 0) exhibit isomorphic structures—represented by identical hash strings—but differ in their embedding activations. We conclude that these predicates are: 1) fundamental building blocks of graph instances, as they are iterated over all structural patterns in the training data, and 2) critical for classification, since the embedding patterns align with the results of the decision tree.

### 3.2 Determining the Logical Structure of $\phi_M$

In this subsection, we aim to construct global logical rules  $\phi_M$  based on hidden predicates  $P$  for each class, which serve the same functionality as the original GNN  $M$ . To achieve this, we adopt a data-driven approach. We process all training instances from class  $c \in C$  that are correctly predicted by  $M$ , evaluating them against the predicates  $P$  and recording their respective activation patterns. The results are stored in a binary matrix  $\Phi_c$  for each class  $c$ , where the columns correspond to the predicates in  $P$ , and the rows represent the training instances correctly classified as  $c$  by  $M$ . Specifically, an entry  $\Phi_c[i, j] = 1$  denotes that the  $j$ -th instance exhibits the  $i$ -th predicate, while  $\Phi_c[i, j] = 0$  indicates otherwise, as illustrated in Figure 1(b).

From a logical structure perspective, each row in  $\Phi_c$  represents a logical rule that describes an instance of class  $c$ , expressed in conjunctive form using hidden predicates. For instance, in the simple binary classification task introduced earlier,  $G_1$  corresponds to the column (1, 1, 0, 1, 0, 0), which can be represented as  $p_1 \wedge p_2 \wedge p_4$ . To derive the global descriptive rules for class  $c$ , denoted as  $\bar{\phi}_M^c$ , we take the disjunction (OR) of all distinct conjunctive forms. Thus, the global rule for our GNN  $M$  in the simple binary classification task, denoted as  $\bar{\phi}_M$ , can be expressed as follows:

$$\forall G, (p_1 \wedge p_2 \wedge p_4) \vee (p_1 \wedge p_5) \Rightarrow \text{label}(G, 0), \quad \forall G, (p_1 \wedge p_2 \wedge p_3) \vee (p_1 \wedge p_3 \wedge p_4 \wedge p_6) \Rightarrow \text{label}(G, 1). \quad (8)$$

Here, we omit  $G$  in  $p_j(G)$  when the context is clear. In addition to the descriptive rules  $\bar{\phi}_M^c$ , we also record the *recurring connectivity patterns* of predicates for each conjunctive form. For instance, in the case of  $(p_1 \wedge p_2 \wedge p_4)$ , both  $p_1$  and  $p_2$  are connected to  $p_4$ , which can be represented using an adjacency matrix. Multiple connectivity patterns may exist, and these can be learned in a data-driven manner, similar to how  $\bar{\phi}_M$  is learned. We denote the collection of connectivity patterns as  $\psi_M$ , which is useful for graph generation and motif-level rule grounding. Additional details on graph generation are provided in Appendix A.11.

To derive an even more compact set of rules that effectively distinguish between classes, we input  $\Phi$  and  $Y$  into a decision tree. The decision tree then identifies the most distinctive and discriminative rules, denoted as  $\hat{\phi}_M$ . For example, in our simple GNN case, the decision tree generates the following discriminative rules:

$$\forall G, \neg p_3(G) \Rightarrow \text{label}(G, 0), \quad \forall G, p_3(G) \Rightarrow \text{label}(G, 1). \quad (9)$$

Note that the discriminative rules  $\hat{\phi}_M$  do not fully replace the descriptive rules  $\bar{\phi}_M$ , as the latter remain valuable for generating graph instances—a task that discriminative rules alone cannot accomplish. Both  $\hat{\phi}_M$  and  $\bar{\phi}_M$  constitute the rules extracted from model  $M$ , collectively denoted as  $\phi_M$ .

### 3.3 Grounding $\phi_M$ into the Input Space

The next challenge is interpreting  $\phi_M$ . To address this, we focus on grounding its building blocks—predicates  $P$ —into the input space  $\mathbf{X}$ , thereby bridging the abstract logic with tangible input features. Recall that a predicate  $p_j$  encodes a subgraph centered on a node  $v$ , encompassing its  $1, \dots, L$ -hop neighborhoods. Each neighbour node is also mapped to some predicate by the predicate function  $f$ . Thus, we can leverage the input features of the node  $v$  along with its neighbour predicates to infer rules that relate the predicate  $p_j$  to the input space. To achieve this, we define the input feature for the

subgraph centered at  $v$  as  $\mathbf{Z}_{v,L}$ , which is constructed by concatenating the information of nodes at each neighborhood level  $l$ :

$$\mathbf{Z}_{v,L} = \text{CONCAT} \left( \mathbf{x}_v, \text{ENCODE} \left( \{f(u) \mid u \in \mathcal{N}^{(1)}(v)\} \right), \dots, \text{ENCODE} \left( \{f(u) \mid u \in \mathcal{N}^{(L)}(v)\} \right) \right) \quad (10)$$

where  $\mathcal{N}^{(l)}(v)$  represents the set of  $l$ -hop neighbors of  $v$ , and ENCODE transforms the collection of predicates into a frequency-based encoding, serving as an order-invariant aggregation operator applied to the predicates of the  $l$ -hop neighbors. For example, as illustrated in Figure 1(c), the subgraph input for node 1 is  $\mathbf{Z}_{1,1} = (1, A, p_4)$ , which indicates that node 1 has a degree of 1 and a type of ‘‘A’’. It also connects to predicate  $p_4$ , representing its sole neighbor, node 2. Similarly, the subgraph input for node 2 is  $\mathbf{Z}_{2,1} = (3, B, p_1, p_1, p_2)$ . Here, we omit the encoding in  $\mathbf{Z}$  for demonstration purposes.

Since model-agnosticism is a key requirement for LOGICXGNN, we approximate the message-passing layers using interpretable models. In this work, we utilize decision trees for this purpose. Specifically, decision trees are employed to generate input-level rules that distinguish predicates with isomorphic subgraphs but different embedding patterns. For this task, the training data for each predicate label  $j$  is the set of subgraph inputs of the nodes  $v$  that activate  $p_j$ , represented as  $\{\mathbf{Z}_{v,L} \mid p_j(v) = 1\}$ . For example, the training data for  $p_1$  (identified as ‘‘cde85e’’, 0) is  $\{\mathbf{Z}_{1,1}, \mathbf{Z}_{3,1}, \dots, \mathbf{Z}_{22,1}\}$ , while the training data for  $p_2$  (identified as ‘‘cde85e’’, 1) is  $\{\mathbf{Z}_{4,1}, \mathbf{Z}_{11,1}, \mathbf{Z}_{20,1}\}$ . The decision tree then generates input-level rules such as  $\mathbf{Z}[1] \leq 0.5$  for  $p_1$ , and the opposite condition for  $p_2$ . Recall that  $\mathbf{Z}[1]$ , i.e., the first dimension of the feature vector  $\mathbf{Z}$ , encodes the node type. Given this, we recognize that  $p_1$  indicates that the node is of type ‘‘A’’, while  $p_2$  indicates that the node is of type ‘‘B’’.

On the other hand, for predicates that do not have an isomorphic counterpart, we simply extract the representative features - this can be selected based on expert knowledge or those with the smallest variance — to explain the corresponding predicates. For instance, for  $p_3$ , supported by  $\{\mathbf{Z}_{18,1}, \mathbf{Z}_{19,1}, \mathbf{Z}_{23,1}, \mathbf{Z}_{24,1}\}$ , the feature with the smallest variance is dimension 0. This indicates that  $p_3$  encodes the fact that the node has a degree of 2. Combining the discriminative rules derived earlier, we yield the following interpretable logic rules  $\hat{\phi}_M$  from the model  $M$ :

$$\forall G, \forall v \in V_G \text{ (degree}(v) \neq 2) \Rightarrow \text{label}(G, 0), \quad \forall G, \exists v \in V_G \text{ (degree}(v) = 2) \Rightarrow \text{label}(G, 1). \quad (11)$$

Sometimes, it is necessary to include neighbor predicates for effective grounding. For instance,  $p_4$ , supported by  $\{\mathbf{Z}_{2,1}, \mathbf{Z}_{12,1}\}$ , encodes the presence of predicate  $p_2$  as a neighbor. Since  $p_2$  encodes type ‘‘B’’,  $p_4$  can be interpreted as having a neighbor node of type ‘‘B’’. By incorporating connectivity patterns  $\psi_M$ , we can generate *motif-level* rules rather than *node-level* through the grounding of adjacent predicates. For example, in our simple GNN case, as shown in Figure 1(c),  $\psi_M$  learns that two instances of  $p_3$  are connected and share connections with the same other predicates. Given that these two nodes corresponding to  $p_3$  have a degree of 2, we can directly infer the following rule:

$$\forall G, \neg \text{has\_cycle}(G) \Rightarrow \text{label}(G, 0), \quad \forall G, \text{has\_cycle}(G) \Rightarrow \text{label}(G, 1), \quad (12)$$

which aligns more closely with human observation, despite the node-level rules are also correct.

### 3.4 Analysis

**Computational complexity** Our approach models message passing at each node in the dataset to identify predicates. In the first step, we extract activation patterns from pretrained GNNs and compute graph hashes on nodes’ local neighborhoods. This step runs independently of the GNN size, with a complexity of  $O(|\mathcal{V}|)$ . Second, determining the logical structure involves constructing a binary matrix of size (number of predicates)  $\times$  (number of graphs), resulting in a complexity of  $O(|\mathcal{V}||\mathcal{G}|)$ . Finally, grounding predicates—by selecting features or performing decision tree analysis for each predicate—has a complexity of  $O(|\mathcal{V}|)$ . We report empirical runtime performance in Table 1.

**Generalization across different GNN architectures** We show the theoretical generalizability of LogicXGNN to any GNN architecture. First, we model stacked message-passing computations using hidden predicates (activation patterns and local subgraphs)—an architecture-agnostic formulation. Next, we generate logic rules through binary matrix construction and decision tree analysis, maintaining architecture independence. Finally, we ground predicates by linking them to input features via decision trees, requiring no GNN-specific details. Empirical evidence is provided in Appendix A.6.

Table 1: Classification accuracy (%) and runtime (seconds) of various explanation methods on benchmark datasets. The first row reports the original GNNs’ accuracy (Runtime is *omitted* for GNNs as comparisons are only relevant for explanation methods). Subsequent rows present results for explanation methods, with the highest accuracy and fastest runtime *among explanation methods* highlighted in bold. Additional evaluations across three random seeds are provided in Appendix A.4.

Method	BAShapes		BBBP		Mutagenicity		NCI1		IMDB	
	Acc.	Time	Acc.	Time	Acc.	Time	Acc.	Time	Acc.	Time
GNN	80.50	–	81.62	–	76.27	–	76.28	–	71.00	–
GLG	57.50	312.7	52.45	359.8	57.95	726.4	53.41	875.74	53.00	329.43
G-TRAIL	82.00	2,543.2	82.11	5,647.9	65.90	20,049.3	66.42	24,067.5	57.50	1,073.4
$\phi_M$ (Ours)	<b>90.00</b>	<b>45.3</b>	<b>83.58</b>	<b>52.8</b>	<b>77.76</b>	<b>103.6</b>	<b>76.03</b>	<b>135.4</b>	<b>65.00</b>	<b>69.5</b>

## 4 Evaluation

In this section, we conduct experimental evaluations on real-world benchmark datasets to address the following research questions:

1. How effective is  $\phi_M$  as a classification tool, especially compared to the original GNN  $M$ ?
2. What knowledge can we derive from the underlying benchmark using  $\phi_M$ ?
3. How effective is  $\phi_M$  as a generative model, and what are its advantages?

**Baselines** Consistent with prior work [2, 3, 30], we focus our comparison on global explanation methods, excluding local approaches such as GNNEXPLAINER [31] due to their differing scope. To benchmark our approach across different functionalities, we use rule-based methods—GRAPHTRAIL [2] and GLGEXPLAINER [3]—as baselines for evaluating classification performance and knowledge extraction. We also include the generation-based method XGNN [32] to benchmark our graph generation ability. All of these methods are considered state-of-the-art. A summary of popular explanation methods and their supported functionalities is provided in Table 2 (Appendix A.1).

**Datasets and Experimental Setup** We use a diverse set of graph classification benchmarks commonly employed in GNN explanation research, with detailed descriptions provided in Appendix A.2. Among these, Mutagenicity [6], NCI1 [25], and BBBP [27] are molecular graph datasets representing chemical compounds; BAMultiShapes [31] is a synthetic dataset focused on structured geometric patterns; and IMDB-BINARY [16] is a social network dataset. To demonstrate the model-agnostic nature of LOGICXGNN, we evaluate it using GCN [10] for BAMultiShapes and BBBP, GraphSAGE [8] for Mutagenicity, GIN [29] for NCI1, and GAT [23] for IMDB-BINARY. Evaluation results for each dataset across various GNN architectures are reported in Table 11. Further details on the experimental setup, including GNN training and baseline implementations, are provided in Appendix A.3.

### 4.1 How effective is $\phi_M$ as a classification tool?

To answer this question, we report the test set classification accuracy of LOGICXGNN ( $\phi_M$ ) against baseline approaches and the original GNN  $M$  in Table 1.

Notably, LOGICXGNN consistently outperforms both baseline approaches—GRAPHTRAIL and GLGEXPLAINER—by a significant margin across all benchmarks. This performance gap can be attributed to fundamental differences in design philosophy. GLGEXPLAINER applies clustering algorithms to local explanations to construct global explanations, while GRAPHTRAIL uses symbolic regression to fit a surrogate rule model on subgraph-level concepts as its explanation. In contrast, LOGICXGNN is designed to model the actual computational flow in GNNs—such as message passing and information pooling—naturally deriving DNF rules as explanations. As a result, both GRAPHTRAIL and GLGEXPLAINER tend to underestimate the complexity of the GNNs’ decision-making process, an issue to which LOGICXGNN is less susceptible. In terms of runtime performance, LOGICXGNN achieves one to two orders of magnitude speedup—approximately 10 to 100 times faster—compared to GLGEXPLAINER and GRAPHTRAIL, by leveraging efficient decision tree algorithms and graph traversal. This eliminates the need for training local surrogate models or performing symbolic regression, significantly reducing computational overhead.

Figure 2: Chemical knowledge extracted by different explanation methods.  $\vee$  and  $\wedge$  represent logical OR and AND, respectively. The symbol  $\dots$  indicates additional patterns that are omitted for brevity.

	Class 0			Class 1		
	LogicXGNN	G-Trail	GLG	LogicXGNN	G-Trail	GLG
Mutagenicity						
BBBP						

Another interesting observation is that  $\phi_M$  can even outperform the original model on certain benchmarks. For instance, on the BAMultiShapes dataset,  $\phi_M$  achieves a test accuracy of 90.00%, significantly surpassing the 80.50% accuracy of the original GNN model  $M$ . This superior performance is also observed and validated in more challenging out-of-distribution scenarios, as discussed in Appendix A.7. Upon closer inspection, we find that LOGICXGNN generally excels on datasets with well-structured, domain-specific patterns, as is often the case with molecular datasets. We believe such datasets may inherently align with a logic-rule-driven structure, allowing GNNs trained on them to exhibit decision-making patterns that can be effectively captured by LOGICXGNN. This demonstrates LOGICXGNN’s potential to replace neural models in scenarios where both high fidelity and interpretability are critical.

However, for graphs with more complex node connections and weaker structural regularities, such as IMDB-BINARY, a performance gap remains. We aim to address this limitation in future work.

#### 4.2 What knowledge can we derive using $\phi_M$ ?

We ground the discriminative rules  $\hat{\phi}_M$  and present the selective biochemical knowledge extracted by LOGICXGNN, as well as by the baseline approaches GLGEXPLAINER and GRAPHTRAIL, for the Mutagenicity and BBBP datasets in Figure 2. Additional results are provided in Appendix A.10.

First, it is worth noting that GLGEXPLAINER cannot independently extract knowledge. It relies on prior domain knowledge to learn concept representations for each cluster of local explanations, which makes it less practical for uncovering unknown knowledge relevant to GNNs’ predictions. Furthermore, we notice both baselines require one-hot encoded inputs. In contrast, our grounding approach makes no assumptions about the input format and even supports continuous features.

Second, we observe that the substructures extracted by LOGICXGNN are chemically accurate and scientifically meaningful, effectively explaining the classification outcomes. For example, we find that molecules containing oxygen-rich functional groups are less likely to cross the blood-brain barrier (Class 0 in BBBP), which can be attributed to their increased hydrophilicity, reduced lipophilicity, and greater likelihood of recognition by efflux transporters [17]. In the context of mutagenicity prediction (with class 0 indicating mutagenic compounds), we not only recover the well-known nitro group ( $\text{NO}_2$ ) attached to aromatic rings—widely recognized for its association with DNA damage and mutagenesis [6, 9]—but also identify other substructures, such as the trichloromethyl group ( $-\text{CCl}_3$ ), which is considered a structural alert for mutagenicity in cheminformatics and toxicology [33].

In contrast, baseline methods tend to extract less relevant or scientifically unsubstantiated substructures, or they identify only a limited subset of patterns that fail to match the breadth and chemical validity of those discovered by LOGICXGNN. For example, GLGEXPLAINER generates merely an  $N-N-N$  substructure for Class 0 in Mutagenicity, accounting for just 38 of 2,463 instances. Similarly, GRAPHTRAIL generates just one pattern for Class 1. This limitation likely explains the observed performance gap between the baseline approaches and LOGICXGNN, as shown in Table 1.

### 4.3 How effective is $\phi_M$ as a generative model?

As the descriptive rules make each decision step in GNNs transparent, they enable accurate modeling of the underlying data distribution and fully controlled instance generation. Specifically, we can select a set of predicates, construct a graph with relevant connectivity patterns learned from the dataset, and apply grounding rules to assign node features, resulting in the final graph. More details on the graph generation process are provided in Appendix A.11. To demonstrate the above merits, we present examples generated by LOGICXGNN and compare the explanation graphs generated by the baseline approach, XGNN, in Figure 3. Figure 9 (Appendix A.11) highlights the diversity in graph generation.

It is worth mentioning that our approach generates new instances that preserve similar structures and key properties, while ensuring adherence to chemical principles such as bonding accuracy. In contrast, XGNN employs a reinforcement learning agent that is inherently black-boxed, producing graphs that do not align with the actual data distribution. For instance, it generates bipartite structures that lack molecular relevance. In summary, LOGICXGNN shows significant potential in fields such as drug design, and we plan to explore these possibilities further in future work.

## 5 Related Work

The explainability of GNNs remains a relatively underexplored area compared to other neural networks, such as convolutional neural networks (CNNs). Most existing methods focus on providing local input attribution explanations [13, 15, 18, 22, 24, 31], similar to attribute-based approaches like Grad-CAM [20] used for explaining CNNs. Another line of research focuses on global explanations that capture the overall behavior of models, which is where our approach, LOGICXGNN, also belongs. Global explanation methods can be broadly divided into generation-based and concept-based approaches. Generation-based methods, such as XGNN [32], use reinforcement learning agents to generate graph instances that maximize specific model predictions. Similarly, GNNInterpreter [26] learns a probabilistic generative graph distribution to produce graph patterns that serve as explanations. These approaches are black-boxed and provide only a limited number of explanation patterns for certain classes, whereas LOGICXGNN is transparent and can generate any desired instance in a controlled manner, making it highly applicable to fields like drug design. On the other hand, concept-based approaches aim to provide more human-readable and precise explanations by leveraging logical formulas and interpretable concepts. For example, GCneuron [30] identifies predefined concepts, formulated as logical combinations of node degrees and neighborhood properties, associated with specific neurons. Similarly, GLGExplainer [3] builds on local explanations from PGExplainer [14], maps them to learned concepts and derives logic formulas from these concepts. GRAPHTRAIL uses symbolic regression to fit a surrogate rule model on subgraph-level concepts as its explanation. In contrast, LOGICXGNN offers a simpler and more intuitive approach, relying solely on decision tree computations rather than complex local explanation methods. It is data-driven, eliminating the need for predefined concepts. Most importantly, while these concept-based approaches typically generate

Figure 3: Selected examples generated by LOGICXGNN and explanation graphs generated by XGNN. Each cell under LOGICXGNN presents the original graph, its corresponding descriptive rules, and a newly generated instance created by modifying those rules. More details are in Appendix A.11.

	LOGICXGNN				XGNN
	Original	Generated	Original	Generated	
BBBP					
	$p_{10} \wedge p_{22} \wedge p_2 \wedge p_{63} \wedge p_{16}$ Class = 1		$p_{16} \wedge p_{12} \wedge p_{26} \wedge p_8 \wedge p_{82} \wedge p_{57} \wedge p_{52} \wedge p_9 \wedge p_{13} \wedge p_{37} \wedge p_{140} \wedge p_{11} \wedge p_{41}$ Class = 1		$p_{12} \wedge p_8 \wedge p_{22} \wedge p_{20} \wedge p_6 \wedge p_{18} \wedge p_{19} \wedge p_{13} \wedge p_6 \wedge p_{11} \wedge p_{41} \wedge p_9 \wedge p_{10}$ Class = 0
Mutagenicity					
	$p_5 \wedge p_2 \wedge p_3 \wedge p_0 \wedge p_4$ Class = 0		$p_{18} \wedge p_{20} \wedge p_4 \wedge p_{20} \wedge p_{15} \wedge p_{28} \wedge p_6 \wedge p_{30} \wedge p_8 \wedge p_{26} \wedge p_{24} \wedge p_5 \wedge p_{17} \wedge p_{32} \wedge p_{22}$ Class = 0		$p_{15} \wedge p_5 \wedge p_{34} \wedge p_{28}$ Class = 1
					max_node = 20, Class = 0
					max_node = 5, Class = 1

descriptive rules for individual classes without distinguishing between them, LOGICXGNN excels in creating discriminative rules that differentiate classes and matches the original model’s accuracy.

## 6 Conclusion, Limitations and Future Work

In this work, we present LOGICXGNN, a novel framework for extracting interpretable logic rules from GNNs. LOGICXGNN is model-agnostic, efficient, and data-driven. More importantly, it can function as a rule-based classifier and even outperform the original neural models. Its interpretability facilitates knowledge discovery, as demonstrated by its ability to extract detailed and chemically accurate insights that are often overlooked by existing methods. A key advantage of LOGICXGNN is its capacity to generate new graph instances in a controlled and transparent manner, offering significant potential for applications such as drug design. However, this also introduces potential risks that must be carefully considered—for instance, the risk of overtrusting the extracted knowledge or generated molcuer graphs without further validation. These risks highlight the need for cautious deployment and expert oversight. While LOGICXGNN outperforms state-of-the-art global explanation methods, a performance gap remains compared to the original GNNs on datasets with more complex node interactions and weaker structural regularities, such as IMDB-BINARY. Addressing this limitation is an important direction for future work. We are also interested in exploring program synthesis on top of LOGICXGNN to further enhance the performance of the rule-based classifier.

## References

- [1] J. Amann, A. Blasimme, E. Vayena, D. Frey, V. I. Madai, and P. consortium. Explainability for artificial intelligence in healthcare: A multidisciplinary perspective. *BMC Medical Informatics and Decision Making*, 20(1):310, Nov 2020. doi: 10.1186/s12911-020-01332-6. URL <https://doi.org/10.1186/s12911-020-01332-6>.
- [2] B. Armgaan, M. Dalmia, S. Medya, and S. Ranu. Graphtrail: Translating GNN predictions into human-interpretable logical rules. In A. Globersons, L. Mackey, D. Belgrave, A. Fan, U. Paquet, J. M. Tomczak, and C. Zhang, editors, *Advances in Neural Information Processing Systems 38: Annual Conference on Neural Information Processing Systems 2024, NeurIPS 2024, Vancouver, BC, Canada, December 10 - 15, 2024*, 2024. URL [http://papers.nips.cc/paper\\_files/paper/2024/hash/df2d51e1d3e899241c5c4c779c1d509f-Abstract-Conference.html](http://papers.nips.cc/paper_files/paper/2024/hash/df2d51e1d3e899241c5c4c779c1d509f-Abstract-Conference.html).
- [3] S. Azzolin, A. Longa, P. Barbiero, P. Liò, and A. Passerini. Global explainability of gnns via logic combination of learned concepts. In *The Eleventh International Conference on Learning Representations, ICLR 2023, Kigali, Rwanda, May 1-5, 2023*. OpenReview.net, 2023. URL <https://openreview.net/forum?id=0TbRTIY4YS>.
- [4] N. Bussmann, P. Giudici, D. Marinelli, and J. Papenbrock. Explainable machine learning in credit risk management. *Comput. Econ.*, 57(1):203–216, Jan. 2021. ISSN 0927-7099. doi: 10.1007/s10614-020-10042-0. URL <https://doi.org/10.1007/s10614-020-10042-0>.
- [5] Z. Chen, F. Silvestri, J. Wang, Y. Zhang, Z. Huang, H. Ahn, and G. Tolomei. Grease: Generate factual and counterfactual explanations for gnn-based recommendations, 2022. URL <https://arxiv.org/abs/2208.04222>.
- [6] A. K. Debnath, R. L. Lopez de Compadre, G. Debnath, A. J. Shusterman, and C. Hansch. Structure-activity relationship of mutagenic aromatic and heteroaromatic nitro compounds. correlation with molecular orbital energies and hydrophobicity. *Journal of Medicinal Chemistry*, 34(2):786–797, 1991. doi: 10.1021/jm00106a046. URL <https://doi.org/10.1021/jm00106a046>.
- [7] C. Geng, X. Xu, Z. Wang, Z. Zhao, and X. Si. Decoding interpretable logic rules from neural networks, 2025. URL <https://arxiv.org/abs/2501.08281>.
- [8] W. L. Hamilton, R. Ying, and J. Leskovec. Inductive representation learning on large graphs, 2018. URL <https://arxiv.org/abs/1706.02216>.
- [9] B. Jin and K. D. Robertson. Dna methyltransferases, dna damage repair, and cancer. *Epigenetic alterations in oncogenesis*, pages 3–29, 2012.
- [10] T. N. Kipf and M. Welling. Semi-supervised classification with graph convolutional networks. In *5th International Conference on Learning Representations, ICLR 2017, Toulon, France, April 24-26, 2017, Conference Track Proceedings*. OpenReview.net, 2017. URL <https://openreview.net/forum?id=SJU4ayYgl>.
- [11] Q. Li, Z. Han, and X. Wu. Deeper insights into graph convolutional networks for semi-supervised learning. In S. A. McIlraith and K. Q. Weinberger, editors, *Proceedings of the Thirty-Second AAAI Conference on Artificial Intelligence, (AAAI-18), the 30th innovative Applications of Artificial Intelligence (IAAI-18), and the 8th AAAI Symposium on Educational Advances in Artificial Intelligence (EAAI-18), New Orleans, Louisiana, USA, February 2-7, 2018*, pages 3538–3545. AAAI Press, 2018. doi: 10.1609/AAAI.V32I1.11604. URL <https://doi.org/10.1609/aaai.v32i1.11604>.
- [12] Y. Liu, Y. Wang, O. Vu, R. Moretti, B. Bodenheimer, J. Meiler, and T. Derr. Interpretable chirality-aware graph neural network for quantitative structure activity relationship modeling. In *The First Learning on Graphs Conference*, 2022. URL <https://openreview.net/forum?id=W20StztdMhc>.
- [13] A. Lucic, M. ter Hoeve, G. Tolomei, M. de Rijke, and F. Silvestri. Cf-gnnexplainer: Counterfactual explanations for graph neural networks, 2022. URL <https://arxiv.org/abs/2102.03322>.
- [14] D. Luo, W. Cheng, D. Xu, W. Yu, B. Zong, H. Chen, and X. Zhang. Parameterized explainer for graph neural network. In H. Larochelle, M. Ranzato, R. Hadsell, M. Balcan, and H. Lin, editors, *Advances in Neural Information Processing Systems 33: Annual Conference on Neural Information Processing Systems 2020, NeurIPS 2020, December 6-12, 2020, virtual*, 2020. URL <https://proceedings.neurips.cc/paper/2020/hash/e37b08dd3015330dccb5d6663667b8b8-Abstract.html>.
- [15] D. Luo, W. Cheng, D. Xu, W. Yu, B. Zong, H. Chen, and X. Zhang. Parameterized explainer for graph neural network, 2020. URL <https://arxiv.org/abs/2011.04573>.

- [16] C. Morris, N. M. Kriege, F. Bause, K. Kersting, P. Mutzel, and M. Neumann. Tudataset: A collection of benchmark datasets for learning with graphs. *CoRR*, abs/2007.08663, 2020. URL <https://arxiv.org/abs/2007.08663>.
- [17] W. M. Pardridge. The blood-brain barrier: bottleneck in brain drug development. *NeuroRx*, 2:3–14, 2005.
- [18] P. E. Pope, S. Kolouri, M. Rostami, C. E. Martin, and H. Hoffmann. Explainability methods for graph convolutional neural networks. In *2019 IEEE/CVF Conference on Computer Vision and Pattern Recognition (CVPR)*, pages 10764–10773, 2019. doi: 10.1109/CVPR.2019.01103.
- [19] S. X. Rao, S. Zhang, Z. Han, Z. Zhang, W. Min, Z. Chen, Y. Shan, Y. Zhao, and C. Zhang. xfraud: explainable fraud transaction detection. *Proceedings of the VLDB Endowment*, 15(3):427–436, Nov. 2021. ISSN 2150-8097. doi: 10.14778/3494124.3494128. URL <http://dx.doi.org/10.14778/3494124.3494128>.
- [20] R. R. Selvaraju, M. Cogswell, A. Das, R. Vedantam, D. Parikh, and D. Batra. Grad-cam: Visual explanations from deep networks via gradient-based localization. In *IEEE International Conference on Computer Vision, ICCV 2017, Venice, Italy, October 22-29, 2017*, pages 618–626. IEEE Computer Society, 2017. doi: 10.1109/ICCV.2017.74. URL <https://doi.org/10.1109/ICCV.2017.74>.
- [21] M. Sun, S. Zhao, C. Gilvary, O. Elemento, J. Zhou, and F. Wang. Graph convolutional networks for computational drug development and discovery. *Briefings in Bioinformatics*, 21(3):919–935, 2020. doi: 10.1093/bib/bbz042.
- [22] J. Tan, S. Geng, Z. Fu, Y. Ge, S. Xu, Y. Li, and Y. Zhang. Learning and evaluating graph neural network explanations based on counterfactual and factual reasoning. In F. Laforest, R. Troncy, E. Simperl, D. Agarwal, A. Gionis, I. Herman, and L. Médini, editors, *WWW ’22: The ACM Web Conference 2022, Virtual Event, Lyon, France, April 25 - 29, 2022*, pages 1018–1027. ACM, 2022. doi: 10.1145/3485447.3511948. URL <https://doi.org/10.1145/3485447.3511948>.
- [23] P. Velickovic, G. Cucurull, A. Casanova, A. Romero, P. Liò, and Y. Bengio. Graph attention networks. In *6th International Conference on Learning Representations, ICLR 2018, Vancouver, BC, Canada, April 30 - May 3, 2018, Conference Track Proceedings*. OpenReview.net, 2018. URL <https://openreview.net/forum?id=rJXMpikCZ>.
- [24] M. N. Vu and M. T. Thai. Pgm-explainer: Probabilistic graphical model explanations for graph neural networks, 2020. URL <https://arxiv.org/abs/2010.05788>.
- [25] N. Wale, I. A. Watson, and G. Karypis. Comparison of descriptor spaces for chemical compound retrieval and classification. *Knowledge and Information Systems*, 14:347–375, 2008.
- [26] X. Wang and H. Shen. Gnninterpreter: A probabilistic generative model-level explanation for graph neural networks. In *The Eleventh International Conference on Learning Representations, ICLR 2023, Kigali, Rwanda, May 1-5, 2023*. OpenReview.net, 2023. URL <https://openreview.net/forum?id=rqq6Dh8t4d>.
- [27] Z. Wu, B. Ramsundar, E. N. Feinberg, J. Gomes, C. Geniesse, A. S. Pappu, K. Leswing, and V. Pande. Moleculenet: A benchmark for molecular machine learning, 2018. URL <https://arxiv.org/abs/1703.00564>.
- [28] J. Xiong, Z. Xiong, K. Chen, H. Jiang, and M. Zheng. Graph neural networks for automated de novo drug design. *Drug Discovery Today*, 26(6):1382–1393, 2021. doi: 10.1016/j.drudis.2021.02.011.
- [29] K. Xu, W. Hu, J. Leskovec, and S. Jegelka. How powerful are graph neural networks? In *7th International Conference on Learning Representations, ICLR 2019, New Orleans, LA, USA, May 6-9, 2019*. OpenReview.net, 2019. URL <https://openreview.net/forum?id=ryGs6iA5Km>.
- [30] H. Xuanyuan, P. Barbiero, D. Georgiev, L. C. Magister, and P. Liò. Global concept-based interpretability for graph neural networks via neuron analysis. In B. Williams, Y. Chen, and J. Neville, editors, *Thirty-Seventh AAAI Conference on Artificial Intelligence, AAAI 2023, Thirty-Fifth Conference on Innovative Applications of Artificial Intelligence, IAAI 2023, Thirteenth Symposium on Educational Advances in Artificial Intelligence, EAAI 2023, Washington, DC, USA, February 7-14, 2023*, pages 10675–10683. AAAI Press, 2023. doi: 10.1609/AAAI.V37I9.26267. URL <https://doi.org/10.1609/aaai.v37i9.26267>.
- [31] R. Ying, D. Bourgeois, J. You, M. Zitnik, and J. Leskovec. Gnnexplainer: Generating explanations for graph neural networks, 2019. URL <https://arxiv.org/abs/1903.03894>.



- [32] H. Yuan, J. Tang, X. Hu, and S. Ji. Xgnn: Towards model-level explanations of graph neural networks. In *Proceedings of the 26th ACM SIGKDD International Conference on Knowledge Discovery & Data Mining*, page 430–438. ACM, Aug. 2020. doi: 10.1145/3394486.3403085. URL <http://dx.doi.org/10.1145/3394486.3403085>.
- [33] E. Zeiger, B. Anderson, S. Haworth, T. Lawlor, and K. Mortelmans. Salmonella mutagenicity tests: Iv. results from the testing of 300 chemicals. *Environmental and molecular mutagenesis*, 11(S12):1–18, 1988.
- [34] Y. Zhang, P. Tiño, A. Leonardis, and K. Tang. A survey on neural network interpretability. *IEEE Trans. Emerg. Top. Comput. Intell.*, 5(5):726–742, 2021. doi: 10.1109/TETCI.2021.3100641. URL <https://doi.org/10.1109/TETCI.2021.3100641>.

## A Appendix

### A.1 Comparison of explanation methods by scope and supported functionalities

Global explanation methods, particularly rule-based ones, are recognized for providing greater explanatory power than local feature attribution methods [34], such as GNNEXPLAINER. For instance, while GNNExplainer computes importance scores for specific substructures such as NO<sub>2</sub> groups and carbon rings in a molecule, our rule-based method confirms their essential and stable role across diverse molecules through logical rules. Consistent with prior work on global explanations (e.g., GRAPHTRAIL, GLGEXPLAINER), we limit comparisons to global baselines, excluding local methods such as GNNEXPLAINER due to their differing scope.

In summary, we compare our approach with several well-known explanation methods in terms of functionality, as outlined below.

Table 2: Comparison of explanation methods by scope and supported functionalities.

Method	Scope	Type	Classification	Knowledge Extraction	Graph Generation
GNNEXPLAINER	Local	Feature Attribution	✗	✗	✗
GCNEURON	Global	Activation-Based	✗	✓	✗
XGNN	Global	Generative	✗	✗	✓
GLGEXPLAINER	Global	Logical Rules	✓	✗	✗
GRAPHTRAIL	Global	Logical Rules	✓	✓	✗
LOGICXGNN	Global	Logical Rules	✓	✓	✓

### A.2 Dataset details

Mutagenicity [6], NCI1 [25], and BBBP [27] are molecular graph datasets, where nodes represent atoms and edges correspond to chemical bonds. In NCI1, each molecular graph is labeled based on its anticancer activity. The Mutagenicity (MUTAG) dataset contains compounds labeled according to their mutagenic effect on the Gram-negative bacterium *Salmonella typhimurium* (Label 0 is mutagenic). In the BBBP dataset, molecules are labeled based on their ability to penetrate the blood-brain barrier. BAMultiShapes [31] is a synthetic dataset consisting of 1,000 Barabási-Albert graphs with randomly placed network motifs, including house, grid, and wheel structures. Class 0 contains plain BA graphs and those augmented with one or more motifs, while Class 1 includes graphs enriched with two motif combinations. IMDB-BINARY [16] is a social network dataset where each graph represents a movie and nodes correspond to actors, with edges indicating co-appearances in scenes. We summarize the statistics of the datasets in Table 3.

Table 3: Statistics of the datasets.

	BAMultiShapes	Mutagenicity	BBBP	NCI1	IMDB-BINARY
#Graphs	1,000	4,337	2,050	4,110	1,000
Avg. $ \mathcal{V} $	40	30.32	23.9	29.87	19.8
Avg. $ \mathcal{E} $	87.00	30.77	51.6	32.30	193.1
#Node features	10	14	9	37	0

### A.3 Experimental setup

All experiments are conducted on an Ubuntu 22.04 LTS machine equipped with 128 GB of RAM and an AMD EPYC™ 7532 processor. Each dataset is split into training and testing sets using an 80/20 ratio. All experiments are repeated using three different random seeds to ensure robustness.

To demonstrate the model-agnostic nature of LOGICXGNN, we employ different GNN architectures across datasets: a 3-layer GCN [10] for BAMultiShapes, a 2-layer GCN for BBBP, a 2-layer GraphSAGE [8] for Mutagenicity, a 3-layer GIN [29] for NCI1, and a 2-layer GAT [23] for IMDB-BINARY.

Figure 4: The screenshot of GLGexplainer github repository. The comment in this code shows that the GLGexplainer remove the graph contains  $NH_2$

```
def read_mutagenicity(explainer="PGExplainer", model="GCN_Tf", split="TRAIN", evaluate_method=True, min_num_include=None, manual_cut=None):
    masked[masked < cut] = 0
    masked[masked >= cut] = 1
    G = nx.from_numpy_matrix(masked)

    connected_components = list(nx.connected_components(G))
    if len(connected_components) == adj.shape[0]: #only single nodes as connected component. No edges in the graph
        continue
    else:
        added = 0
        for cc in connected_components:
            if len(cc) >= 2: #to exclude single nodes
                G1 = G.subgraph(cc)
                if len(G1.nodes()) >= len(G.nodes()) - 3:
                    continue

            nodes_to_keep = list(G1.nodes())
            #to_keep = embedding[nodes_to_keep]
            to_keep = features[nodes_to_keep]
            for n in nodes_to_keep:
                G1.nodes[n]["atom_type"] = features[n].argmax(-1)

            pattern_found = False
            for i, pattern in enumerate([pattern_nh2, pattern_no2]):
                if pattern_found:
                    continue
                GM = isomorphism.GraphMatcher(G1,
                                                pattern,
                                                node_match=isomorphism.categorical_node_match(['atom_type'], [0]))
                if GM.subgraph_is_isomorphic():
                    pattern_found = True
                    le_classes.append(i)
            if not pattern_found:
                le_classes.append(2)
            if le_classes[-1] == 0: #tempary remove class 0 since there is just 1 example
                del le_classes[-1]
            continue

        added += 1
        adjs.append(nx.to_numpy_matrix(G1))
        edge_weights.append(nx.get_edge_attributes(G1, "weight"))
```

For training, we use the Adam optimizer with a learning rate of 0.005. Training proceeds for up to 500 epochs, with early stopping after a 100-epoch warm-up if validation accuracy does not improve for 50 consecutive epochs. All explainers are evaluated on the test split.

Additionally, we use the CART algorithm to construct the decision trees in LOGICXGNN. For baseline approaches, we adopt the authors' original implementations and follow their recommended hyperparameters to ensure a fair comparison.

**Reproducibility analysis of GLGEXPLAINER** We reproduced the results of GLGEXPLAINER [3] using the official GitHub repository, but encountered several challenges that raise concerns about the fairness of direct comparisons, many of which were also reported by GRAPHTRAIL [2]

First, although GLGEXPLAINER relies on PGEXPLAINER [14] to generate local explanations (i.e., important subgraphs), the public codebase only includes precomputed outputs rather than the implementation for invoking PGEXPLAINER. This omission prevents the method from being directly applied—using the authors' original parameters—to additional datasets beyond those used in the original paper. As a result, we conducted our own trials on other datasets.

Second, GLGEXPLAINER requires prior domain knowledge to learn concept representations for each cluster of local explanations produced by PGEXPLAINER. It also performs dataset-level filtering to exclude graphs that are less relevant to this domain knowledge. For example, in the MUTAG dataset, it relies on the assumption that nitro groups ( $NO_2$ ) and amines ( $NH_2$ ) are indicative of mutagenicity. Based on this assumption, it filters out molecules that do not contain these functional groups, as illustrated in Figure 4.

In this code snippet, GLGEXPLAINER excludes the following types of graphs:

- Graphs whose important subgraphs are nearly as large as the original graph,
- Graphs with overly simplistic explanations (e.g., single-edge motifs),
- Graphs containing unique patterns (e.g., the only graph with an  $\text{NH}_2$  group).

These filtering criteria introduce bias by favoring instances with clear and frequent motifs, potentially overstating the model’s performance. In contrast, our method and GRAPHTRAIL make no such assumptions and operate without relying on prior domain knowledge.

Third, while the paper claims to use the elbow method to threshold edge importance scores, we found that for the MUTAG dataset, a fixed, hard-coded threshold was used instead. This inconsistency suggests possible cherry-picking and weakens reproducibility.

To ensure a fair comparison, we re-ran GLGEXPLAINER with the elbow method enabled and all graph-level filtering disabled, ensuring that all methods were evaluated on the same test set. Under these conditions, GLGEXPLAINER exhibited a significant performance drop compared to the original results reported in [3]. Our reproduced results are consistent with those reported in [2].

#### A.4 Additional experiments on classification

To ensure robust and reliable performance, we conduct additional evaluations of runtime and accuracy using three random seeds. The mean and standard deviation are reported in Table 4 and Table 5, respectively. We also report weighted precision, recall, and F1-score, averaged across the three runs, in Table 6, Table 7, and Table 8, respectively. The highest accuracy and fastest runtime *among explanation methods* are highlighted in bold.

Table 4: Runtime (seconds) on graph classification datasets.

Method	BAShapes	BBBP	Mutagenicity	NCI1	IMDB
GLG	272.6 $\pm$ 31.7	329.3 $\pm$ 46.8	744.0 $\pm$ 59.2	883.7 $\pm$ 74.5	336.6 $\pm$ 42.2
G-TRAIL	2,676.2 $\pm$ 124.5	5,418.9 $\pm$ 534.7	20,167.0 $\pm$ 1,047.9	25,226.1 $\pm$ 1,435.7	1,103.7 $\pm$ 67.3
$\phi_M$ (Ours)	<b>50.7 <math>\pm</math> 5.8</b>	<b>47.5 <math>\pm</math> 7.4</b>	<b>104.7 <math>\pm</math> 13.5</b>	<b>127.6 <math>\pm</math> 15.2</b>	<b>67.2 <math>\pm</math> 2.9</b>

Table 5: Test accuracy (%) on graph classification datasets.

Method	BAShapes	BBBP	Mutagenicity	NCI1	IMDB
GNN	81.00 $\pm$ 0.41	83.33 $\pm$ 1.31	74.81 $\pm$ 1.23	75.18 $\pm$ 1.63	71.83 $\pm$ 1.43
GLG	58.83 $\pm$ 1.43	52.42 $\pm$ 1.03	57.90 $\pm$ 1.73	54.46 $\pm$ 1.85	53.83 $\pm$ 1.43
G-TRAIL	81.00 $\pm$ 0.41	81.13 $\pm$ 0.92	65.63 $\pm$ 0.69	66.67 $\pm$ 2.20	56.83 $\pm$ 0.62
$\phi_M$ (Ours)	<b>91.00 <math>\pm</math> 1.41</b>	<b>85.13 <math>\pm</math> 2.20</b>	<b>76.35 <math>\pm</math> 1.35</b>	<b>74.74 <math>\pm</math> 2.12</b>	<b>65.67 <math>\pm</math> 2.09</b>

Table 6: Weighted precision (%) on graph classification datasets.

Method	BAShapes	BBBP	Mutagenicity	NCI1	IMDB
GNN	79.27 $\pm$ 1.44	82.30 $\pm$ 1.75	75.34 $\pm$ 0.98	75.19 $\pm$ 1.62	71.85 $\pm$ 1.43
GLG	58.87 $\pm$ 1.24	53.56 $\pm$ 0.62	58.48 $\pm$ 1.71	54.47 $\pm$ 1.84	53.89 $\pm$ 1.18
G-TRAIL	81.72 $\pm$ 0.60	79.08 $\pm$ 1.31	69.50 $\pm$ 1.32	67.06 $\pm$ 2.22	61.60 $\pm$ 1.82
$\phi_M$ (Ours)	<b>92.04 <math>\pm</math> 1.10</b>	<b>84.34 <math>\pm</math> 2.44</b>	<b>76.41 <math>\pm</math> 1.44</b>	<b>74.76 <math>\pm</math> 2.13</b>	<b>70.84 <math>\pm</math> 2.72</b>

Table 7: Weighted recall (%) on graph classification datasets.

Method	BAShapes	BBBP	Mutagenicity	NCI1	IMDB
GNN	78.83 $\pm$ 1.70	83.33 $\pm$ 1.31	74.81 $\pm$ 1.23	75.18 $\pm$ 1.62	71.83 $\pm$ 1.43
GLG	58.83 $\pm$ 1.43	52.42 $\pm$ 1.03	57.90 $\pm$ 1.73	54.46 $\pm$ 1.85	53.83 $\pm$ 1.43
G-TRAIL	81.00 $\pm$ 0.41	81.13 $\pm$ 0.92	65.63 $\pm$ 0.69	66.67 $\pm$ 2.20	56.83 $\pm$ 0.62
$\phi_M$ (Ours)	<b>91.00 <math>\pm</math> 1.41</b>	<b>85.13 <math>\pm</math> 2.20</b>	<b>76.35 <math>\pm</math> 1.35</b>	<b>74.74 <math>\pm</math> 2.12</b>	<b>65.67 <math>\pm</math> 2.09</b>

Table 8: Weighted F1-score (%) on graph classification datasets.

Method	BAShapes	BBBP	Mutagenicity	NCI1	IMDB
GNN	78.64 $\pm$ 1.80	81.86 $\pm$ 1.35	74.24 $\pm$ 1.34	75.18 $\pm$ 1.62	71.79 $\pm$ 1.38
GLG	58.73 $\pm$ 1.32	48.41 $\pm$ 1.09	58.02 $\pm$ 1.72	54.46 $\pm$ 1.84	53.74 $\pm$ 1.33
G-TRAIL	80.77 $\pm$ 0.38	78.55 $\pm$ 0.98	61.56 $\pm$ 0.68	66.40 $\pm$ 2.25	48.65 $\pm$ 0.91
$\phi_M$ (Ours)	<b>90.89 <math>\pm</math> 1.45</b>	<b>84.24 <math>\pm</math> 2.34</b>	<b>76.29 <math>\pm</math> 1.44</b>	<b>74.73 <math>\pm</math> 2.12</b>	<b>63.44 <math>\pm</math> 1.33</b>

### A.5 Evaluating LOGICXGNN performance on additional datasets

We evaluate the performance of LOGICXGNN on additional graph classification datasets to further support our claim that:

- LOGICXGNN can outperform original GNNs on datasets with well-structured, domain-specific patterns.
- However, in cases with weaker structural regularities, there remains a performance gap between LOGICXGNN and original GNNs.

To this end, we train GCNs on the HIN [3], PROTEINS [16], and AIDS [16] datasets, with dataset statistics summarized in Table 10. Among these, HIN represents a face-to-face interaction network collected in a hospital environment, PROTEINS contains large and complex compounds related to enzymes, and AIDS consists of molecular graphs labeled according to anti-HIV activity. Notably, HIN and PROTEINS exhibit weaker structural regularities, whereas AIDS contains clearer, well-defined patterns. Our results in Table 9 further reinforce our claim. Addressing the performance gap on datasets with weaker structural signals is left as an important direction for future work.

Table 9: Test accuracy (%) on additional datasets.

Method	HIN	PROTEINS	AIDS
GNN	85.04 $\pm$ 0.58	70.85 $\pm$ 0.37	81.17 $\pm$ 0.82
G-TRAIL	50.57 $\pm$ 0.61	58.74 $\pm$ 1.32	87.25 $\pm$ 0.54
$\phi_M$ (Ours)	<b>78.98 <math>\pm</math> 1.29</b>	<b>63.97 <math>\pm</math> 0.84</b>	<b>94.25 <math>\pm</math> 0.94</b>

Table 10: Statistics of the additional datasets.

	HIN	PROTEINS	AIDS
#Graphs	1,760	1,113	2,000
Avg. $ \mathcal{V} $	11.68	39.1	15.69
Avg. $ \mathcal{E} $	36.06	145.6	32.39
#Node features	5	3	38

Table 11: Evaluation of LOGICXGNN across different GNN architectures, measured by classification accuracy (%).  $M$  and  $\phi_M$  denote the original GNN model and its corresponding LOGICXGNN-based explanation, respectively. The higher accuracy in each pair is bolded.

Dataset	GCN [10]		GraphSAGE [8]		GIN [29]		GAT [23]	
	$M$	$\phi_M$	$M$	$\phi_M$	$M$	$\phi_M$	$M$	$\phi_M$
BAShapes	79.00	<b>90.50</b>	47.00	<b>47.00</b>	92.00	<b>93.50</b>	47.00	<b>47.00</b>
BBBP	79.41	<b>83.33</b>	82.60	<b>84.31</b>	81.86	<b>82.60</b>	<b>83.58</b>	83.33
Mutagenicity	76.04	<b>76.50</b>	76.27	<b>77.65</b>	80.07	<b>80.07</b>	76.04	<b>77.53</b>
IMDB	<b>71.50</b>	65.50	<b>73.00</b>	66.50	<b>73.50</b>	66.50	<b>71.00</b>	65.00
NCI1	<b>69.95</b>	69.34	<b>72.26</b>	70.68	<b>76.28</b>	76.03	<b>70.56</b>	69.83

### A.6 Empirical evidence for generalizability across GNN architectures

In Table 11, we present the robustness of LOGICXGNN compared to the original GNN models across various architectures. LOGICXGNN consistently achieves high classification accuracy and

even outperforms its neural counterparts in several scenarios. These results further substantiate the strong performance of LOGICXGNN in preserving predictive quality while providing interpretable explanations.

### A.7 Evaluating LOGICXGNN performance on challenging out-of-distribution scenarios

To further supports our claim that rule-based models can perform as well as trained GNNs, we evaluate LOGICXGNN on more challenging out-of-distribution (OOD) scenarios. To this end, we implemented Murcko scaffold splitting with an 80:20 train-test ratio, repeated across three different random seeds. Table 12 reports the mean and standard deviation of test accuracies. Our evaluation uses datasets from MoleculeNet, where SMILES strings are available for scaffold computation.

Table 12: Test accuracy (%) under Murcko scaffold-based splitting on MoleculeNet datasets. Results are reported as mean  $\pm$  standard deviation over three runs.

Model	BACE	BBBP	SIDER
GNN	72.34 $\pm$ 1.18	82.52 $\pm$ 0.84	74.01 $\pm$ 0.85
LOGICXGNN	<b>74.22</b> $\pm$ 1.66	<b>84.71</b> $\pm$ 0.93	<b>76.11</b> $\pm$ 1.13

Notably, LOGICXGNN outperforms the original GNN by a certain margin in this OOD setting compared to the random-split scenario. This suggests that LOGICXGNN effectively captures the underlying logic governing GNN predictions. We further hypothesize that many graph tasks—particularly those involving molecules—may naturally align with logic-rule structures, which are not always well approximated by conventional GNNs. In future work, we plan to explore program synthesis approaches built upon LOGICXGNN to uncover such rule-based patterns.

### A.8 Rule Stability under Perturbations

We assess the robustness of extracted rules by conducting 5-fold cross-validation on multiple graph datasets, as reported in Table 13. In each fold, we independently extract rules and compared the logical forms (conjunctive clauses) against those from the baseline fold. Across all datasets, we observe a high overlap in rule structures—between 88% and 96%—demonstrating strong consistency.

This high rule matching confirms that LOGICXGNN identifies stable, semantically meaningful patterns in the GNN’s decision process. Rather than overfitting to specific training samples, our method uncovers fundamental relational logic that persists across data splits, which is essential for building trust in explainable AI systems.

Table 13: 5-fold cross-validation accuracy (%) and rule overlap (%) with fold 1.

Dataset	Fold 1	Fold 2	Fold 3	Fold 4	Fold 5
BAMultiShapes	88.00 (–)	86.50 (95.67)	86.25 (93.75)	87.50 (96.15)	86.00 (94.23)
Mutagenicity	76.50 (–)	75.46 (93.15)	76.15 (91.78)	75.12 (94.52)	76.61 (93.97)
BBBP	81.37 (–)	80.39 (88.10)	83.09 (92.86)	81.13 (95.24)	80.15 (90.48)

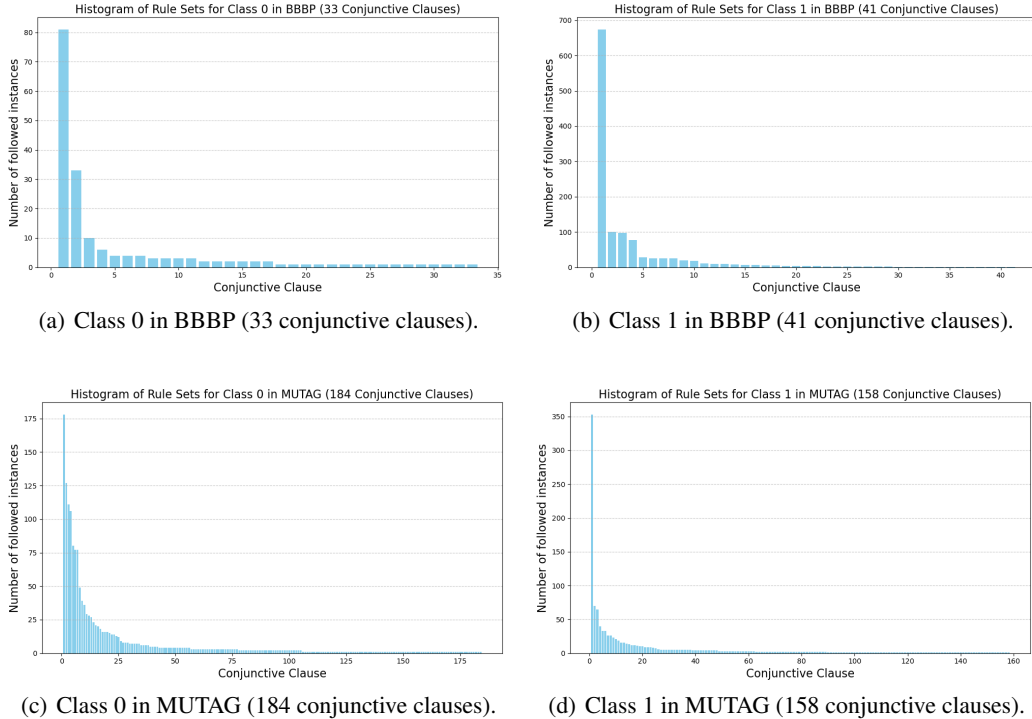
Table 14: Node classification accuracy (%) on heterogeneous graph datasets.

Method	Cora	PubMed
GNN	78.23	<b>81.41</b>
LOGICXGNN	<b>80.44</b>	80.63

### A.9 Evaluating LOGICXGNN on node classification

Our approach naturally extends to node classification tasks, as it models message passing at the node level. This setting is currently unsupported by existing global explainers. We report results on two heterogeneous datasets in Table 14.

Figure 5: Histograms showing the number of instances covered by each conjunctive clause in the rule sets extracted by LOGICXGNN for the BBBP and MUTAG datasets.



#### A.10 More details on knowledge extraction

We provide additional details on our knowledge extraction experiments in Section 4.2. Table 15 presents the number of extracted conjunctive clauses (patterns) for each class across different methods. Notably, LOGICXGNN captures a diverse set of patterns that better reflect the intricate decision-making processes of GNNs, while baseline methods (GLGEXPLAINER and GRAPHTRAIL) tend to underestimate this complexity.

We present complete rule sets produced by baseline approaches on Mutagenicity and BBBP in Figure 6. In comparison, LOGICXGNN generates more diverse patterns, as quantified in Table 15 (e.g., 184 and 158 patterns for Class 0 and Class 1 in Mutagenicity, respectively). We report only the top 10 most representative conjunctive clauses in Figure 7, all of which are scientifically meaningful and help explain GNNs’ prediction outcomes. Selected patterns appear in the main paper (Figure 2).

Although our approach produces a large number of patterns, we observe that only a small subset of them dominate in terms of coverage, explaining the majority of graph instances. Many of the remaining patterns are highly specific and account for only a few instances, as shown in Figure 5.

Table 15: Number of extracted conjunctive clauses (patterns) for each class using different methods.

Dataset	Class 0			Class 1		
	$\phi_M$ (Ours)	G-TRAIL	GLG	$\phi_M$ (Ours)	G-TRAIL	GLG
Mutagenicity	184	5	1	158	1	1
BBBP	33	1	5	41	2	3

Figure 6: Complete rules produced by baseline approaches for MUTAG and BBBP.

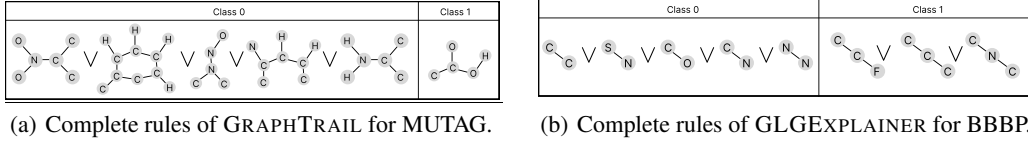
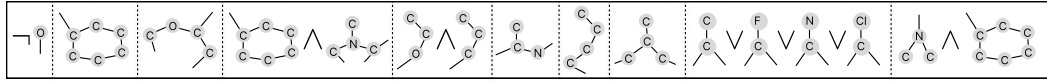
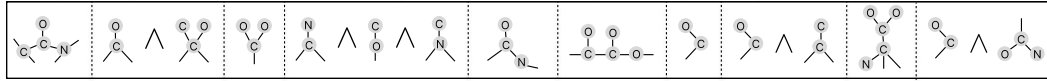
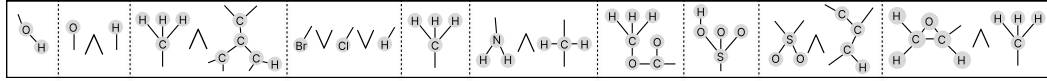
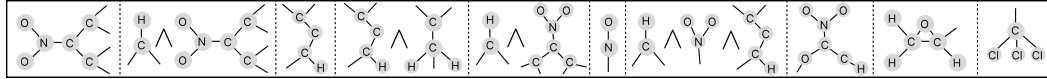


Figure 7: Top 10 most representative conjunctive clauses (patterns) extracted by LOGICXGNN for the MUTAG and BBBP datasets. Each pattern appears in a dedicated cell, with clauses combined via logical OR operators to form the classification rules.




---

**Algorithm 1:** Graph Instance Generation

---

**Input:** Descriptive rules ( $\bar{\phi}_M$ ), connectivity patterns ( $\psi_M$ ), predicate grounding rule ( $R$ )  
**Output:** A graph  $G = (V, E)$  with node features  $X_V$

```

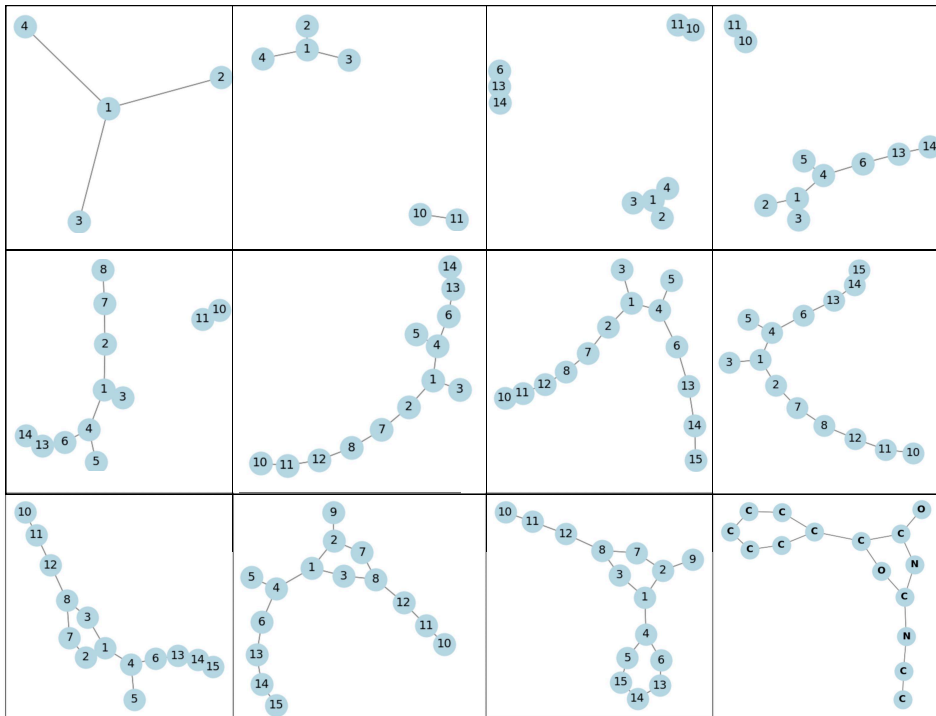
1 Function generateGraph( $\bar{\phi}_M, \psi_M, R$ )
2    $C \leftarrow \text{Sample}(\bar{\phi}_M)$  /* Sample a conjugate clause  $C$  */
3    $\text{Template} \leftarrow \psi_M(C)$  /* Extract connectivity patterns regarding  $C$  */
4    $E \leftarrow \emptyset, V_{\text{dict}} \leftarrow \{\}$  /* Initialize edges and nodes */
5   for  $\text{tmp} \in \text{Template}$  do
6      $\text{node\_freq} \leftarrow \text{CountNodeFrequencies}(\text{tmp})$  /* Compute node frequency */
7      $V_{\text{dict}} \leftarrow \text{UpdateNodes}(\text{tmp}, V_{\text{dict}}, \text{node\_freq})$  /* Update node dictionary */
8      $(\text{node}, \text{first\_neighbors}, \text{second\_neighbors}) \leftarrow \text{tmp}$  /* Unpack pattern tuple */
9      $\text{node\_picked} \leftarrow \text{Sample}(V_{\text{dict}}[\text{node}])$  /* Select a node randomly */
10     $\text{neighbors\_picked} \leftarrow \text{PickFirstNeighbors}(\text{first\_neighbors}, \text{node\_picked}, V_{\text{dict}})$ 
11    for  $j \in \text{neighbors\_picked}$  do
12       $E \leftarrow E \cup \{(\text{node\_picked}, j)\}$ 
13       $E \leftarrow E \cup \{(j, \text{node\_picked})\}$  /* Add bidirectional edges */
14   $X_V \leftarrow R(V_{\text{dict}}, E)$  /* Apply grounding rule once graph generation completes */
15  return  $(V_{\text{dict}}, E), X_V$ 

```

---



Figure 8: A step-by-step example. From subfigure (1,1) to (3,3), we incrementally add subgraphs corresponding to the selected predicates and connect them based on the provided connectivity patterns. The final subfigure (3,4) shows the grounding phase, where each node is assigned an atom number.



### A.11 LOGICXGNN as Generative Model

As LOGICXGNN makes each decision-making step in GNNs transparent with descriptive rules, we can leverage LOGICXGNN as a generative model for creating graph instances in a controlled manner.

More specifically, our approach enables diverse graph generation through three key steps: (1) constructing predicate collections as building blocks, (2) selecting blueprints from the connectivity pattern pool, and (3) applying grounding preferences. Recall that predicates serve as the fundamental building blocks, while connectivity patterns act as blueprints that guide their composition into the final graph. Algorithm 1 details this procedure, and Figure 8 provides a step-by-step real-world example for clarity. More graph generation examples are shown in Figure 9, where multiple different molecular graphs are generated based on input molecules.

**Graph Generation from Known Instances: Instructions for Figure 3 and Figure 9** In this setting, we first extract descriptive rules from input molecules. These rules are then modified—by adding or removing predicates—and used to construct graphs based on relevant connectivity patterns learned from the full dataset. Finally, we apply the learned grounding rules to generate the corresponding molecular structures. For instance, consider cell (1,1) in Figure 3. The original descriptive rule is  $p_{10} \wedge p_{22} \wedge p_2 \wedge p_{63} \wedge p_{16}$ . We simplify it to  $p_{10} \wedge p_{63} \wedge p_{16}$  to match the following connectivity pattern found in the bank of relevant structures:  $p_{16}$  is connected to  $p_{63}$ ;  $p_{63}$  is connected to  $p_{10}$ ; and  $p_{10}$  is connected to both  $p_{10}$  and  $p_{63}$ . Finally, we apply a grounding rule where  $p_{63}$ ,  $p_{10}$ , and  $p_{16}$  correspond to motifs composed of carbon atoms. Based on this configuration, we successfully generate a new molecule. Each of these three steps introduces potential variations, yet all remain fully transparent and interpretable—offering a significant advantage over black-box generative approaches such as diffusion models.

This generation process highlights the transparency and controllability of our system from an end-user perspective. A more systematic study and quantitative comparison with state-of-the-art generative methods is left for future work, as a comprehensive exploration of the generative capabilities would exceed the scope of this 9-page paper.

Figure 9: Selected examples generated by descriptive rules  $\bar{\phi}_M$ . The first three rows display results for BBBP, and the bottom three rows show results for Mutagenicity. The first column represents the original graph, while each cell in the remaining columns presents a newly generated graph derived from it.

